AD 296 507

RADC-TDR - 62 - 324 JANUARY 2, 1963

296 507

MULTIPLE TAPPED PHOTOELASTIC DELAY LINE

FINAL REPORT, PHASE 1
JUNE 1, 1961 - JUNE 1, 1962

CORNING ELECTRONICS
CORNING GLASS WORKS
550 HIGH STREET
BRADFORD, PENNSYLVANIA

CONTRACT NUMBER

AF 30 (602) - 2060

PREPARED FOR

ROME AIR DEVELOPMENT CENTER
AIR FORCE SYSTEMS COMMAND
GRIFFISS AIR FORCE BASE
NEW YORK

CORNING
ELECTRONICS

RADC - TDR - 62 - 324 JANUARY 2, 1963

MULTIPLE TAPPED PHOTOELASTIC DELAY LINE

FINAL REPORT, PHASE 1

CORNING ELECTRONICS
CORNING GLASS WORKS
550 HIGH STREET
BRADFORD, PENNSYLVANIA

CONTRACT NUMBER
AF 30 (602) - 2060

PROJECT NUMBER
4506

TASK NUMBER
45359

PREPARED FOR

ROME AIR DEVELOPMENT CENTER
AIR FORCE SYSTEMS COMMAND
GRIFFISS AIR FORCE BASE
NEW YORK

Copy No. 39

CORNING ELECTRONICS

ABSTRACT

This report is concerned with an optical technique for detecting an acoustic signal in a glass ultrasonic delay line. A useful model with a system bandwidth of 10 mc centered at 15 mc, a signal-to-noise ratio exceeding 20 db and five independent outputs separated one from another by 0.1 usec has been constructed and is described herein. Having built a model with these characteristics, it is possible to determine both the advantages and the feasibility of ultimately producing a multiple tapped delay line with as many as 1000 taps.

AUTHORIZATION

The work described in this report was performed by the Delay Line Research & Development Department of the Corning Glass Works and the report was prepared by I. C. Miller, A. J. Polucci and G. J. Pratt.

This project is directed and administered by the Rome Air Development Center, Air Force Systems Command, U. S. Air Force under Contract AF30-(602)-2060.

Submitted by:

G. J. Pratt
Project Leader

Approved by:

R. J. Stone
R. J. Stone
Supervisor

TABLE OF CONTENTS

TABLE OF CONTENTS (CONT'D)

LIST OF FIGURES

I INTRODUCTION

A. Background

Detection of the signal in a solid transparent ultrasonic delay line by photoelastic means was described by Arenberg[1] in 1948. Wilmotte[2] later conducted an extensive investigation of the processes of modulation of light by ultrasonic means, employing both the photoelastic properties of glasses and the Debye-Sears diffraction effect. This work was done in connection with the development of an instantaneous cross-correlator and it was concluded that the photoelastic system was more useful. Wilmotte reported that modulation of a light beam could be obtained at 400 kilocycles per second. The results at a modulating frequency of 2.5 megacycles per second were not entirely satisfactory although there was no apparent reason why much higher frequencies could not be used.

Using the above references as a foundation, Brouneus and Jenkins[3] successfully extended the operating frequency to 30 mc and compared the relative merits of utilizing the shear and compressional modes.

The work described in this report is an outgrowth of an RADC Contract awarded to Corning Glass Works in 1959 which called for feasibility studies of multiple-tapped ultrasonic delay lines. Corning

and RADC subsequently narrowed the effort to the photoelastic approach as being the most promising.

To establish the advantages and feasibility of ultimately producing a delay line having 1000 taps, it was decided that a working model with at least five taps should be designed and constructed. This model would crystalize previous work and the specifications, encourage development of theory and techniques to extend the performance and make the photoelastic delay line a more practical device.

B. Specifications for Model

Center frequency	$\approx$ 15 mc
Overall bandwidth	$>$ 10 mc
Number of taps	5
Tap separation	0.1 usec
Signal to noise ratio @ 50% light modulation	$>$ 20 db
Maximum delay	100 usec
Signal output voltage into 93 ohms	$>$ 50 millivolts

C. Format of Report

Since the theory describing optical detection of acoustic signals is well covered in the references, our aim here is to emphasize specific engineering accomplishments. Design features of the model

are justified wherever possible by reference to theory. In many instances only qualitative explanations are available to substantiate experimental results, however, these ideas should serve as the basis for more rigorous experimental work in this area.

D. Contribution of the Wiley Electronics Company

As part of this contract, the Wiley Electronics Company of Phoenix, Arizona was requested to design and construct a solid state 15 mc amplifier to be used in conjunction with the photomultiplier detector. In addition, as an independent check on our own work, they investigated means for improving the signal-to-noise ratio and performed noise measurements with a line identical to the one supplied by Corning to RADC as part of the model.

A final report from Wiley Electronics is submitted, along with this report, describing their results.

II PRINCIPLES OF OPERATION

A. The Shear Mode Photoelastic Light Modulator

The system for modulating light and obtaining time delay by means of the photoelastic effect consists of, with reference to Figure I, the following basic elements in the order given:

a. A source of light and means for collimation.

b. A polaroid-plate acting as a polarizer of the incident light with the axis of the major transmittance oriented at an angle of 90° to the sonic wave front in the photoelastic delay line (item d. below).

c. A phase delay plate for converting the plane polarized light to circularly polarized light. At the operating optical wavelength, each of the two components of the circularly polarized light is parallel to a stress axis in the glass. A phase delay plate having $\lambda/4$ relative delay at a wavelength of 5400 $\mathring{A}$ was used in the experimental set up.

d. A photoelastic delay line in the form of a fused silica bar with a high efficiency PZT transducer operating in the thickness shear mode bonded to one

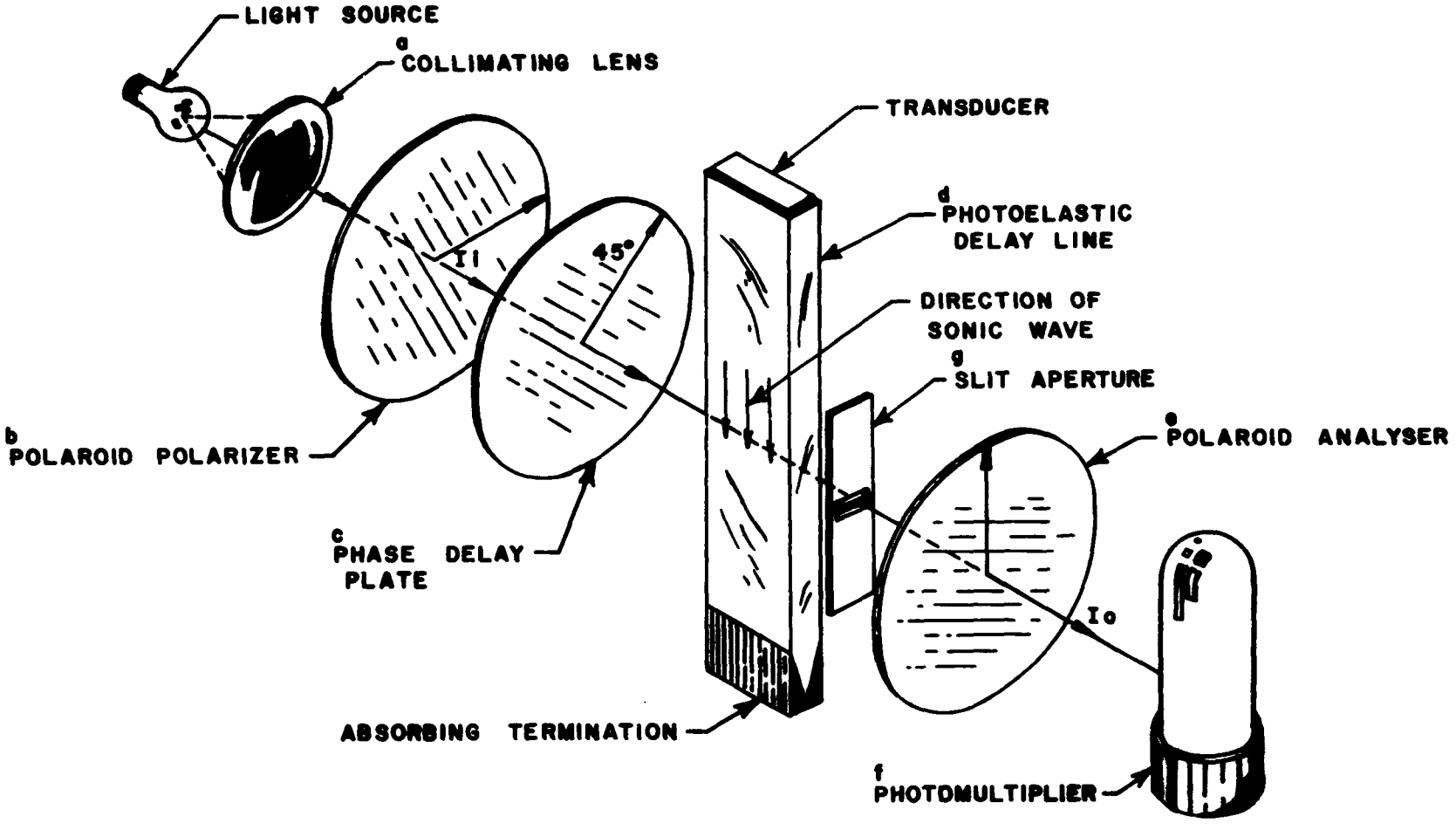

Fig. I Basic Elements of a Photoelastic Delay System

end. At the end opposite the transducer facet an acoustic terminator can be located to attenuate any reflected energy to a level of better than 50 db below the incident energy.

e. A second polaroid-plate acting as an analyzer with the axis of major transmittance oriented at a right angle to the major axis of the first polaroid (a.).

f. A suitable photoelectric pickup for converting the emergent modulated light into a usable electrical signal.

g. A narrow slit (or slits) parallel to the sonic wave-front and inserted in the optical path. The slit width is adjusted to some fraction of the acoustic wavelength; $\lambda_0/3$ being the desirable width for our purposes.

B. The Modulation Process

Modulation of light by the photoelastic delay line occurs in the following manner:

When an alternating electric signal is applied to the delay line transducer a sonic wave is propagated the length of the delay line. As the wave passes any given point, that point alternately undergoes tension and compression along the principle stress axis. The incident circularly polarized light is therefore modified. Upon

emerging from the photoelastic delay line the relative phase delay between the two components of the circularly polarized light will be greater or less than 90° depending on the instantaneous stress in the delay line at that point. The light alternating between circular and elliptical polarization is analyzed by the second polaroid plate or analyzer. This results in a final emergent light intensity which varies in direct accord with the instantaneous polarity and amplitude of the original electrical signal applied to the delay line transducer.

Figure II illustrates the response of the optical system just described as a function of the phase difference γ between the two components of the light passing through the delay line bar. It can be shown [4] that $\frac{\text{Intensity Out}}{\text{Intensity In}}$ is proportional to $\text{Sin}^2 \frac{\gamma}{2}$

By inserting a quarter wave plate $\left(\gamma = \frac{\pi}{2}\right)$ between the polarizer and analyzer the operating point of the system is fixed at the point of most linear response, and as shown a sinusoidal variation in phase difference will result in a sinusoidal variation in output light intensity. Percentage light modulation is the ratio of $\frac{Ia}{Ib}$, as defined in the figure.

C. Basic Considerations

1. Transducer Size

For a given percentage light modulation and transducer width held constant, (a.) the power required to drive the transducer is inversely proportional to the optical path or the transducer

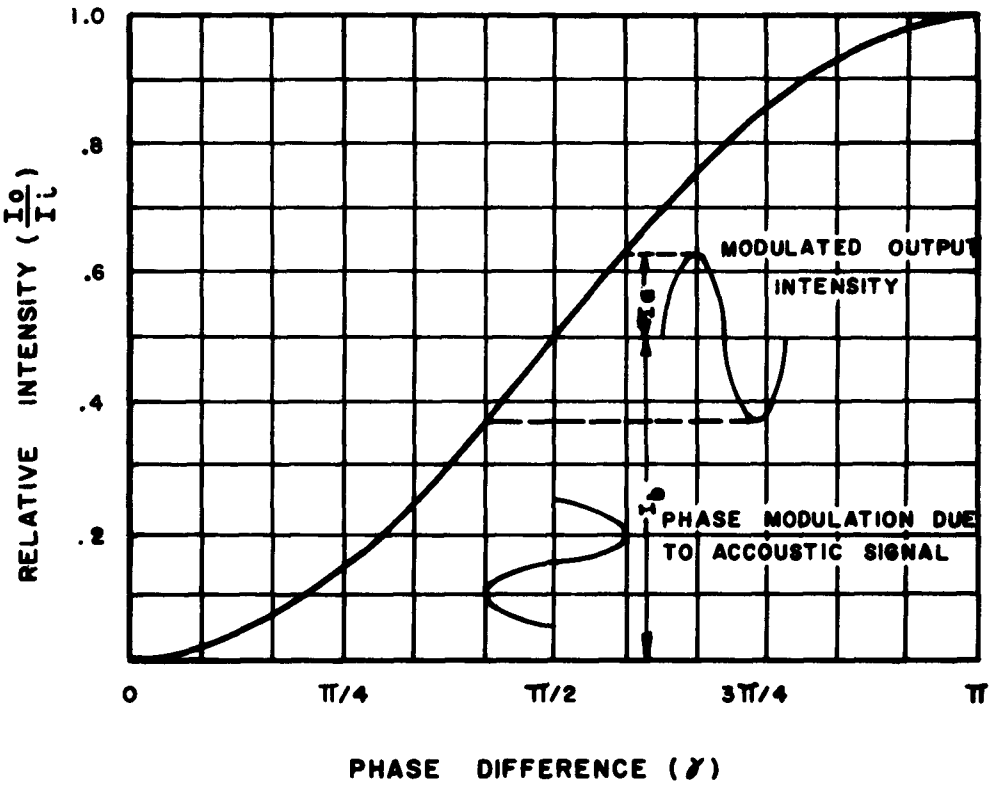

Fig. II Response of Optical System

length and (b.) the power dissipated per unit area is inversely proportional to the square of the transducer length. Also, if the transducer length is doubled, the drive voltage required to maintain a given percentage modulation will be halved.

It is therefore advantageous to use the longest practical transducer from a drive power point of view.

2. Signal to Noise Ratio

It can be shown * that the ratio of the output rms signal current to the rms noise current at the output is given by

$$\frac{i^2}{i_n^2} = \frac{S}{N} = K \frac{(\alpha \beta I_b \lambda_o d)}{(\Delta f) e} \left[m \frac{\sin \pi \alpha}{\pi \alpha} \right]^2$$

where α = $\frac{\text{slit width}}{\text{acoustic wavelength}}$

λ_o = acoustic wavelength

I_b = light bias intensity

Δf = electrical bandwidth of detector plus following circuitry

d = length of optical slit

β = photomultiplier cathode efficiency

e = electron charge

m = % light modulation

K = dimensionless constant

* See Appendix B and reference (5).

Considering α alone, maximum S/N ratio results when $\alpha = .37\lambda_0$, however, this ratio is relatively insensitive to slit width variation from $\frac{\lambda_0}{4}$ to $\frac{\lambda_0}{2}$ as can be seen by plotting $\alpha\left[\frac{\sin \pi\alpha}{\pi\alpha}\right]^2$

The product $\alpha\beta I_b \lambda_0 d$ simply represents the DC photomultiplier cathode current and the product $m\frac{\sin \pi\alpha}{\pi\alpha}$ represents the percentage modulation of the cathode current.

Considering the dependence of the S/N ratio on the overall bandpass, it should be noted that it is independent of the delay line bandpass and for an optimum ratio the detector bandpass should be kept as small as possible.

In our work the detector bandpass was restricted to 9 mc and an overall bandpass of 10 mc was achieved by appropriate shaping of the response of the delay line and driving circuitry.

3. Slit Width

There are four excellent reasons why the optimum slit width is less than one half wavelength at the center frequency.

a.) Signal Level

Considering the photomultiplier cathode current to be the signal, for a half wave slit the percentage signal modulation is only 63% of the percentage light modulation. As the slit-width is reduced to zero, the percentage signal

modulation approaches the percentage light modulation but the signal itself goes to zero. Thus for a given operating anode current (determined by the tube gain), maximum signal voltage output will result when the slit width is made as small as possible and the tube gain is increased accordingly.

b.) S/N Ratio

As indicated previously, maximum signal to noise ratio results (using a photomultiplier type photodetector) when the slit width is .37 λ_o . This ratio is relatively insensitive to small variations of slit width about this value but falls off rapidly below a slit width of .2 λ_o .

c.) Bandpass

The slit response falls off as $\frac{\sin \pi a}{\pi a}$, therefore, as the slit width approaches zero, the slit bandwidth approaches infinity. To minimize skewing of the overall bandpass, the slit width should be as small as possible, consistent with other requirements.

d.) Tube Fatigue

By using the smallest slit width consistent with the desired performance characteristics, the DC light flux through the slit is minimized, insuring the maximum possible stability of the cathode surface. Dynode fatigue,

however, will still be dependent on the operating anode current.

Considering the above, the variation in light output when light sources are changed, the gain characteristics of the photomultiplier, and the amount of light available, we adopted a slit width of .3 λ at 15 mc for use with the model.

4. Choice of Component Parts for the Model

In our work the over-riding consideration was that the cathode current - which for a given bandwidth and percentage light modulation essentially determines the S/N ratio - be made as large as possible. For this reason an intense arc lamp was chosen for the light source and a lens of short focal length was used as the collimator. In addition, the photomultiplier was chosen primarily on the basis of its cathode sensitivity.

5. Circuitry Associated with the Photomultiplier

When it is necessary that the photomultiplier tube be located at a distance from a succeeding amplifier or oscilloscope, the shunt capacitance reactance of the connecting cable will seriously reduce the high frequency sensitivity. For this reason an impedance transformer in the form of a cathode-follower amplifier succeeds each of the five photomultipliers.

The high input impedance of the cathode-follower allows a

lower value of load impedance in the photomultiplier anode circuit while providing ample sensitivity with anode currents well within the ratings of the photomultiplier tube.

III DESCRIPTION OF SYSTEM

A. Description of Model

Figures III and IV shows the final version of the model furnished Rome Air Development Center.

To the left of the optical bench are three power supplies with a ballast resistor panel which supply power for the DC operated arc lamp, the five photomultiplier tubes and the five cathode followers.

The light housing at the extreme left on the optical bench supports a 100 watt mercury arc lamp. A 100 usec fused silica delay line is mounted on a traversing mechanism which enables continuous variation in delay. To the left of the delay line is an 8" focal length collimating lens and HNCP37 circular polarizer combined in such a way to provide adjustment of both lens position and polarizer orientation. To the right of the delay line is the fiber optic head (See Figure VII) with six optical slits attached and a disk of HNCP37 which acts as the analyzer. Five of the six fiber bundles conduct modulated light to five RCA 7764 photomultipliers mounted in the readout chassis. Any one of the five voltage outputs from the cathode follower may be examined conveniently on the dual trace scope by use of the channel selector mounted at the right end of the optical bench. Signal outputs from all followers may be displayed or further processed

Fig. III General View of Photoelastic Delay System

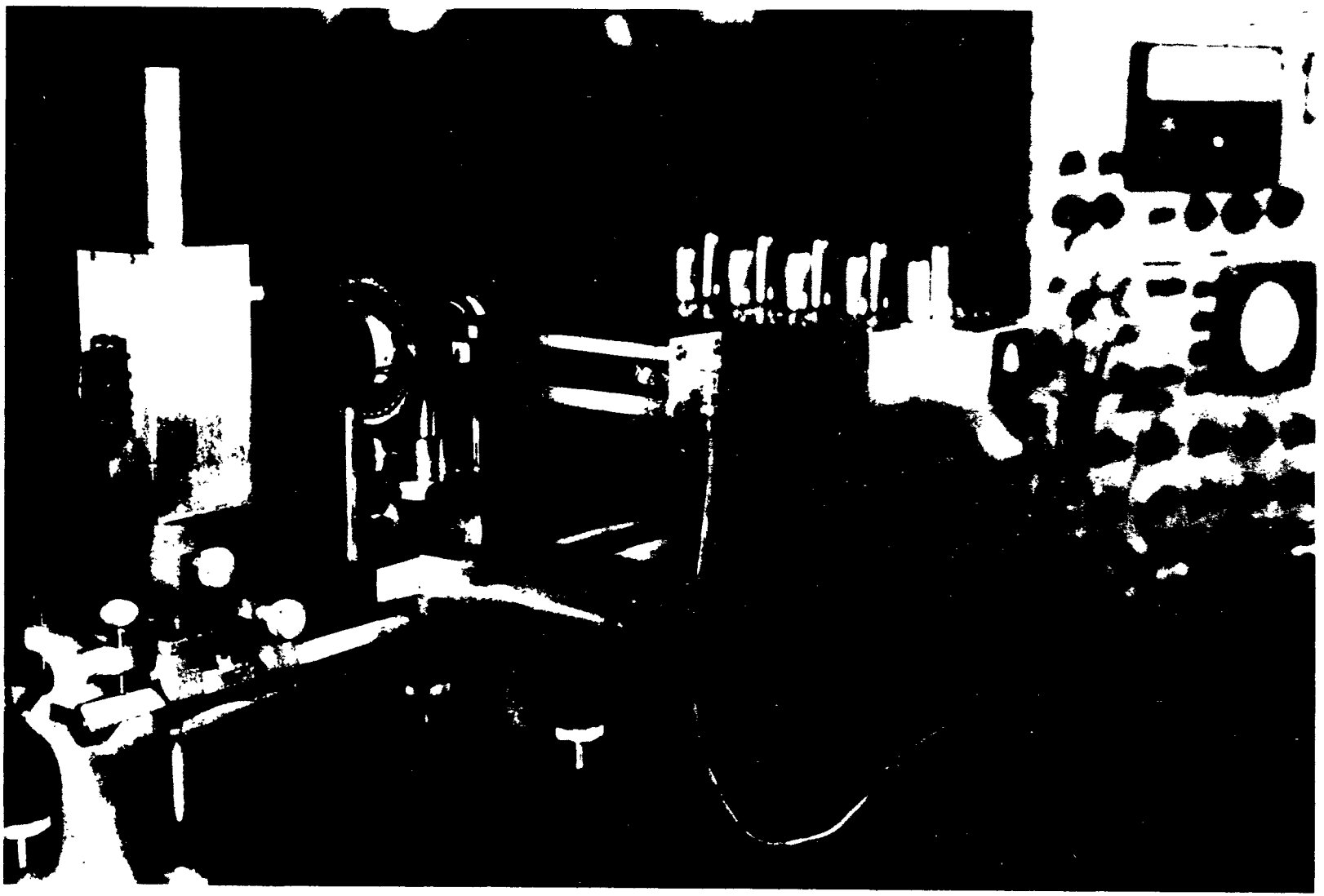

Fig. IV Close-up View of Delay Line and Traversing Mechanism

simultaneously if desired. Atop the oscilloscope is an Arenberg pulsed oscillator model 650C which is used for driving the delay line.

The model is so designed that it is possible to operate it in ambient room light without degradation of performance.

B. Performance of Model

1. Final measurements of signal level and system bandwidth of the five channels are shown in Figure V. The alignment of optical components was in accordance with procedures described in the instruction manual previously supplied with the model.

The 3 db bandwidths were between 10 and 11 mc/s on all five channels, and output signal voltages were 50 millivolts or more with photomultiplier anode currents of 150 microamperes.

2. Delay time measurements with the readout head set near the center of the bar were made:

Channel	Delay Time sec	Time Difference μ sec
1	47.618	
		.091
2	47.709	
		.091
3	47.800	
		.091
4	47.890	
		.091
5	47.980	

Figure VI is a photograph of the output pulses obtained from the five

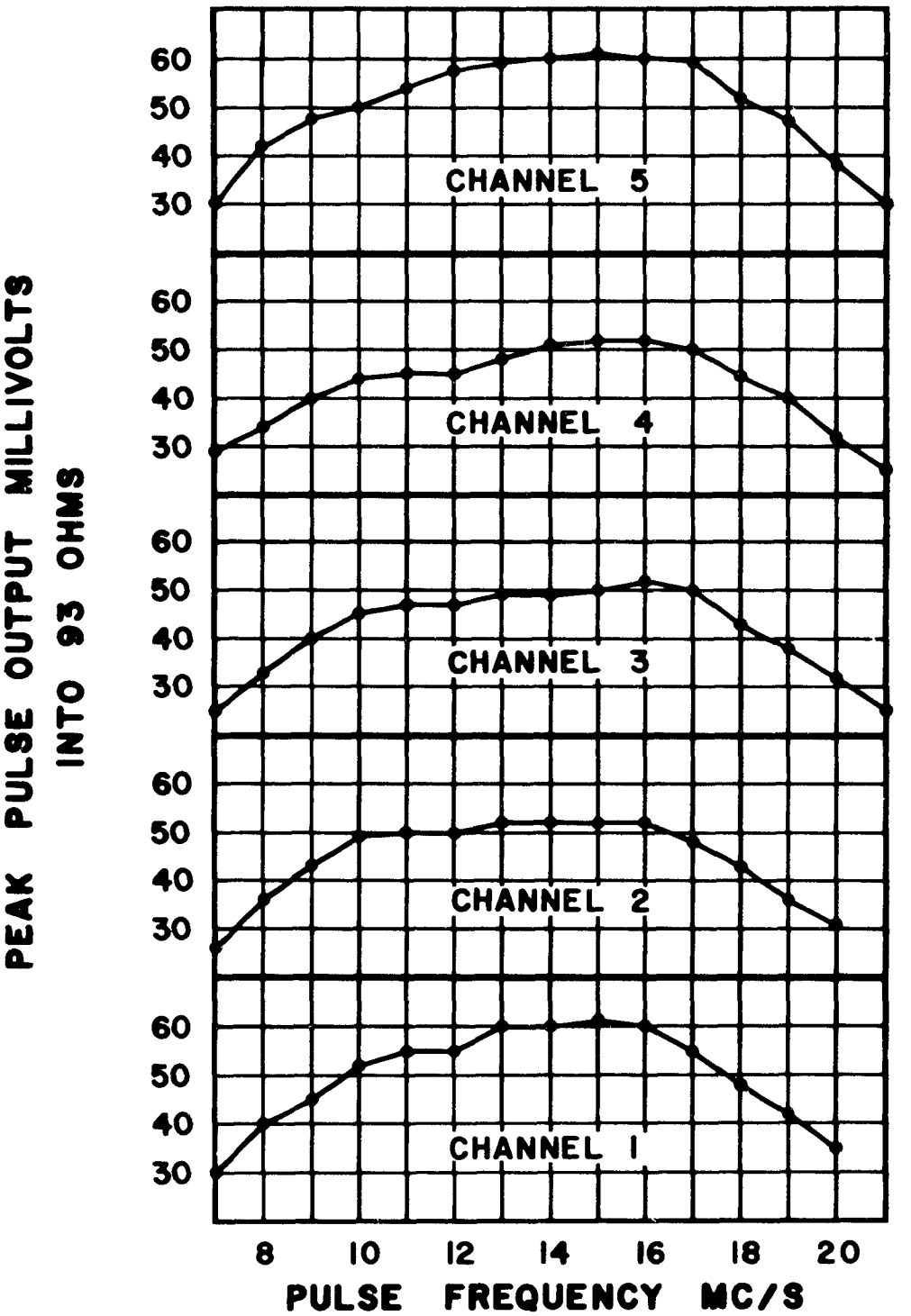

Fig. V System Frequency Response

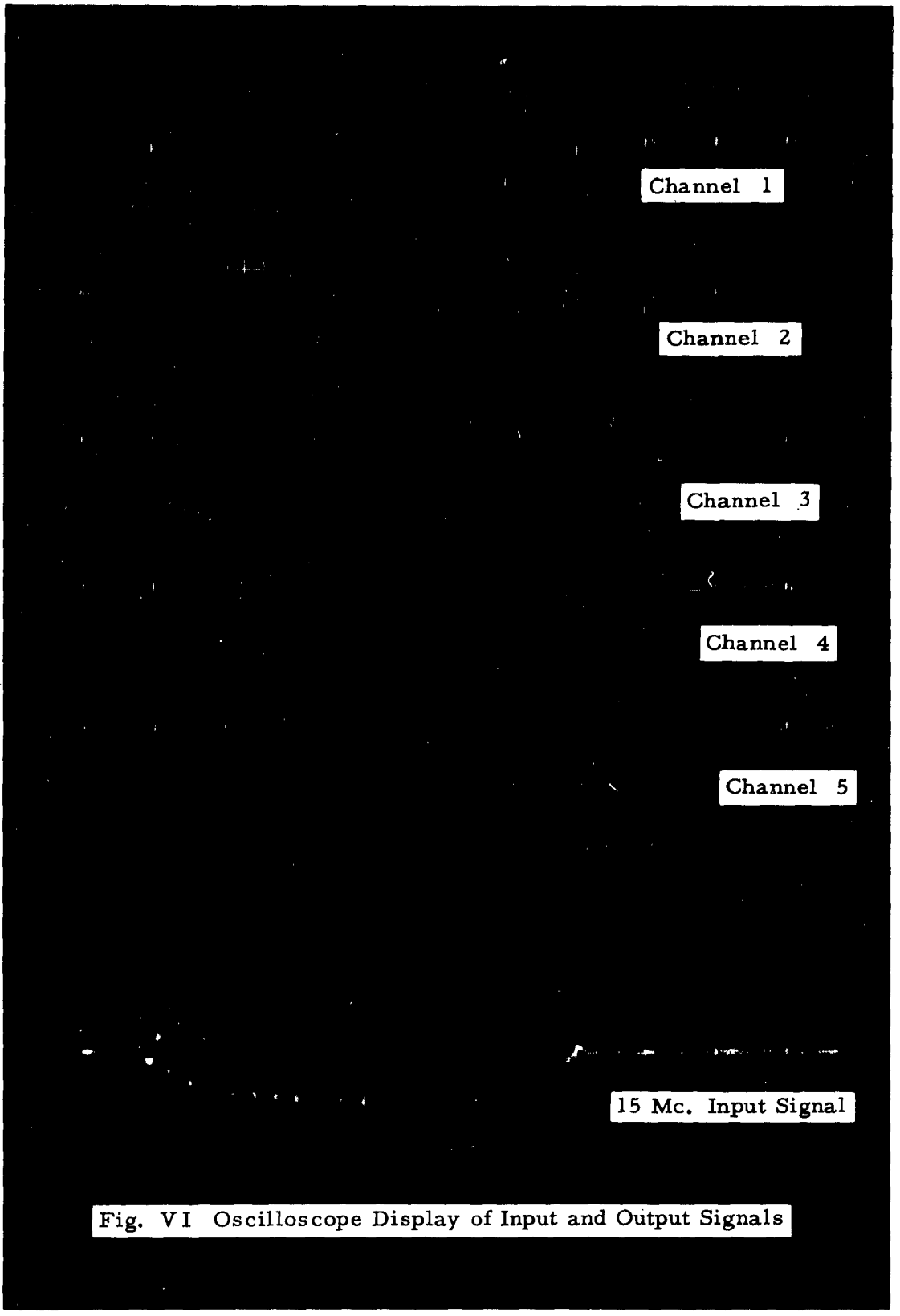

Fig. V I Oscilloscope Display of Input and Output Signals

taps. The undelayed input pulse is also shown at the bottom of the photo. The carrier frequency of the pulse is 15 mc/s. Sweep speed in the photograph is 0.2 usec/cm. Superimposed input and delayed pulses of equal amplitude were not photographed, because it was virtually impossible to distinguish the display from a single pulse trace.

3. Phase shift vs. frequency was examined over the frequency range from 7 to 21 mc/s. Data was obtained by measuring time delay of each tap at one megacycle intervals, 7 through 21 mc/s.

The time change vs. frequency was normalized around 15 mc/s, (arbitrarily assigning a value of $\Delta T = 0$ usec at 15 mc, i.e. $\phi = 0$). Time delay change at each other frequency was converted to degrees at the frequency of measurement. The maximum positive and negative phase change was calculated to be 30°.

Because of substantial scattering of plot points, the method was re-examined, and it was concluded that the time delay measurement accuracy is inadequate, particularly on the high frequency side of 15 mc/s. One nanosecond at 20 mc/s is equal to 7.2° of phase and our equipment is presently limited to $\pm$ 3 nanoseconds. However, less than 45° phase shift across the passband appears to be a certainty.

4. The voltage required for 100% light modulation was determined by increasing the transducer drive voltage to obtain maximum

output signal.

It can be seen from Figure II that the drive voltage required for 50% light modulation is one third the voltage necessary for 100% light modulation, when the transducer and the optical path length remain unchanged. This was demonstrated experimentally.

Peak voltage required at the transducer at 15 mc/s for 50% modulation is 4.5 volts. Peak power to the transducer is approximately 7 watts. Required voltage at the input to the transducer frequency compensating network is 15 volts, and peak pulse power to the network and transducer is approximately 22 watts for 50% light modulation.

5. Signal amplitude at several frequencies from 12 to 16 mcs/s was observed while scanning the length of the optical delay line. Output voltage was relatively constant throughout the 15 inch length of the line. Output voltage fall off from transducer to distant end of the line was less than 2 db at 16 mc/s. At 12mc/s the roll off was 4 db, implying beam spreading as the probable cause.

The line had been tested for signal amplitude vs readout position prior to optical flatting and polishing and wide variations in output voltage were noted. Considerable improvement resulted from the optical polishing.

IV DISCUSSION OF COMPONENT PARTS

1. Light Source and Collimating Lens

An Osram 100W1 high pressure mercury arc was used as the light source. This DC operated lamp emits approximately 2000 lumens when operated at the rated power of 100 watts. The arc dimensions are .3 mm x .3 mm and this is sufficiently small so that for our immediate application, condensing lenses and a source slit are not required.

A 1.5" diameter f8 plano convex lens was used as the collimating lens and afforded uniform illumination over 1.5" of delay line path length. With this simple combination of light source and collimating lens, a variable multiple-tapped delay line having approximately 100 independent outputs separated in delay one from another by 0.1 usec could be fabricated if the need justified the effort.

Difficulty was experienced with some of the Osram lamps used for experimental work due to the rapid shifting of the arc strike points on the electrodes. In extreme cases the light flicker was actually visible to the unaided eye. This shifting of the arc position resulted in a fluctuation in the output signal level and delay time. Selected Osram 100W1 lamps perform adequately for something

less than the rated lifetime of 100 hours.

2. Photodetectors

Solid state detectors were initially considered because of their small size; however, frequency, bandwidth, signal level and noise requirements precluded their usage during this phase of the contract. In general, the frequency response of a well designed photomultiplier is flat up to about 100 megacycles above which the variation in electron transit time becomes the limiting factor. For these reasons two RCA photomultipliers were evaluated for use with the model: the 7764 with an Sl 1 spectral response and the 1P21 with an S-4 response.

Despite the fact that the 7764 has twice the cathode sensitivity in the visible region, peaks 400 Å lower than the 1P21 and was operated at rated voltage, the S/N ratios obtained with these tubes were essentially the same under identical conditions of illumination, bandwidth, and tube gains. The 1P21 was operated at a gain of only 3000 (so as not to exceed the maximum anode current rating of 100 u amps) by reducing the bleeder supply voltage to about 250 volts.

The 7764 rather than the 1P21 was chosen for use with the model, because the maximum anode current which is five times that of the 1P21, enables greater output signal voltage levels. Its lower anode to ground capacitance permits use of a greater load impedance

for th same bandwidth. In addition, the stability of the 7764 is far superior to that of the 1P21 for the anode currents that we worked at.

In the report by Wiley Electronics a cathode surface having an S4 response is compared with one having an S17 response. The conclusion is that with a mercury arc source, the S17 cathode appears to be about twice as sensitive as an S4 cathode. An increase in cathode sensitivity by a factor of two would increase the S/N ratio by 3 db.

3. Optical Components

Other things remaining constant, the phase difference introduced by a given stress in the glass is directly proportional the frequency of the light. It would be desirable therefore to operate in the far blue or ultraviolet regions of the spectrum from a drive power standpoint; however, the transmission characteristics of present fiber optic bundles limit the useful light frequencies to those of the visible region centered about green.

HNCP37 circularly polarizes light at 5400 $\mathring{A}$ and in general was found to be at least as good as any combination of the various polaroid materials.

Optimization of the S/N ratio demands that the D. C. cathode current be made as large as possible. Involved here is the matching of a light source spectral output with the transmission characteristics of the polarizing material, quarter wave plate, fused silica delay line,

fiber optic bundles, and photomultiplier window with the response of the photo cathode. This was not done as part of the contract because of time limitations, so it is difficult to estimate what improvement could be realized in the signal to noise ratio by better matching of the spectral responses of the individual optical components.

The transmission and efficiency of the polarizing elements could be improved by use of crystal optics but it is felt that ultimately polaroid will be required when it is necessary to illuminate the entire delay line.

4. Fiber Optic Tapping Device

Tapping of the delay line is accomplished by use of the fiber optic device shown in Figure VII. Six independent bundles or channels are provided. Made up of 15 micron fibers, the overall transmission of each bundle is better than 55% at 5461 Å.

The end view of the head shows the configuration of the apertures as seen by the delay line. The bundle width of .0148" determines the tap spacing of .1 usec since .0148" of delay line path length represents .1 usec of delay. A photographic mask containing six slit apertures separated one from another by .0148" and having a clear width of $\lambda_o/3$ (.0033" at 15 mc) is cemented to the head to establish precise tap spacing and aperture width.

The fiber optic assembly was fabricated by the Bausch and

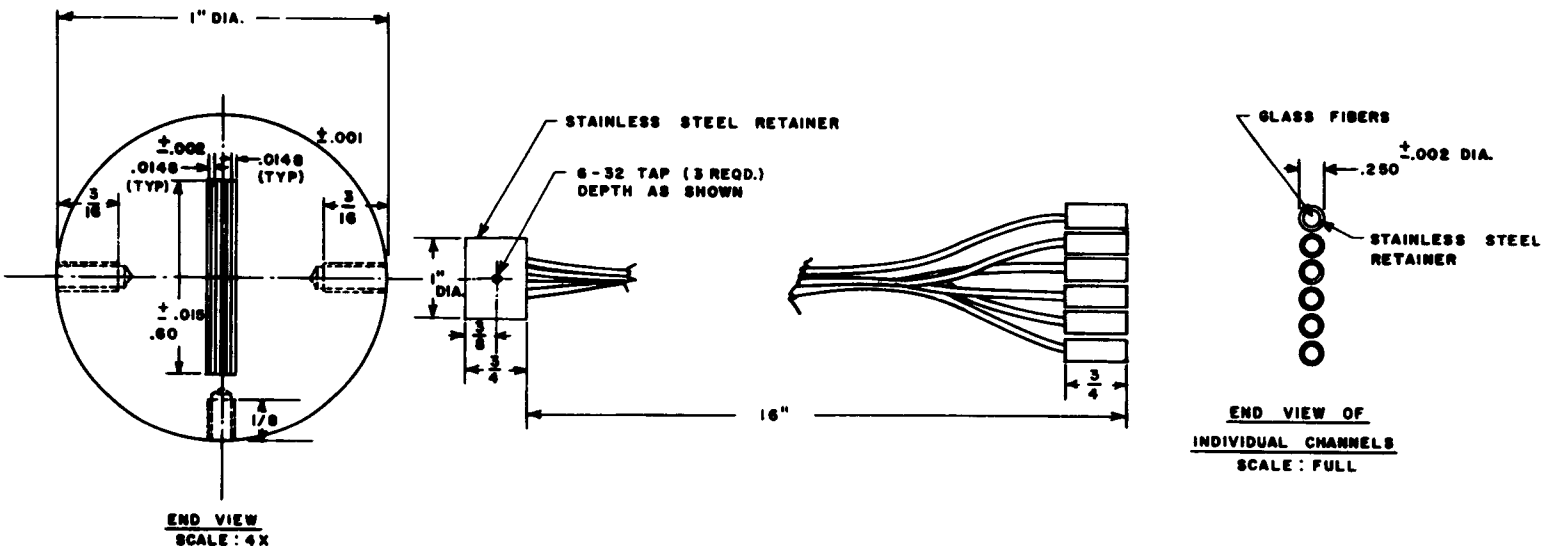

NOTES:

1. TRANSMISSION OF EACH BUNDLE MUST BE AT LEAST 55% AT 5461 Å.
2. THERE MUST BE NO CROSS TALK BETWEEN CHANNELS.
3. BUNDLE ENDS ARE TO HAVE AN OPTICAL FINISH.
4. FIBER DIAMETER 15 MICRONS
5. BUNDLE ENDS TO BE FLUSH WITH RETAINERS.

CORNING GLASS WORKS
DRAWING NO. 13368-4262

Fig. VII Fiber Optic Six Channel Tapping Device

Lomb Company of Rochester, New York, and performs admirably well.

5. Transducer

The transducer is comprised of six 15 mc/s shear wafers bonded to the optically flat 7/8" x 2" transducer facet, as shown in Figure VIII. Non-loading back electrodes were formed by evaporation of a gold film over the wafers. Subsequent masking and sandblasting completed the six 0.3"x 5/8" electrodes.

The six sections were series connected (in phase) to reduce capacitance and increase the radiation resistance to manageable values. A capacitance of 2000 picofarads and a radiation resistance of slightly less than 3 ohms were measured at 15 mc.

A thicker delay line with a wider transducer would permit the use of a longer optical slit which would admit more light to the photomultiplier and result in a better signal-to-noise ratio. Transducer area and drive power requirements would increase proportionately and transducer impedance would become impractically low.

The configuration and dimensions of the PZT-2 transducer are a reasonable design compromise, providing adequate signal-to-noise ratio at moderate power levels and manageable input impedance.

New transducer ferroceramics now under development hold promise of more compatable characteristics.

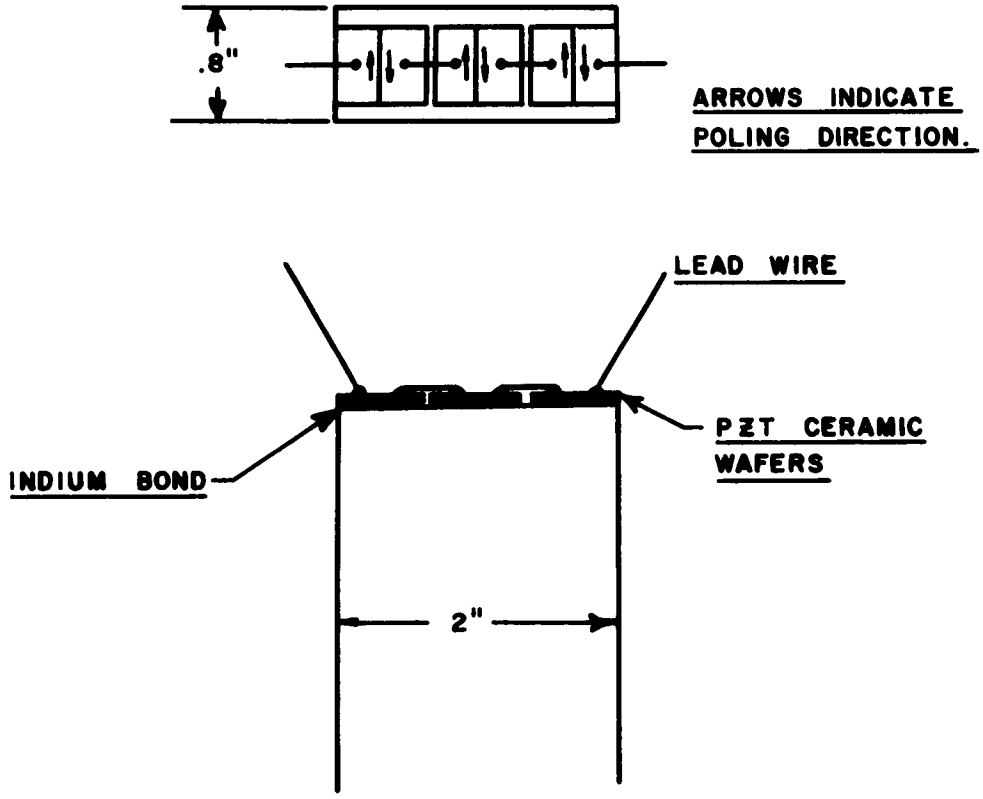

Fig. VIII Delay Line Transducer Assembly

6. Photomultiplier & Output Circuitry

Dual (cascaded) cathode followers transfer the photomultiplier signal voltage developed across its anode load to a low impedance output. The input follower was designed to operate with a large transfer constant (approx. 0. 94), to minimize asymmetry of pulse reproduction and the adverse effects on photomultiplier bandwidths of tube (grid) capacitance. Direct interstage and output coupling provides very wide interstage bandwidth and rapid recovery from D. C. transients produced by light intensity changes.

Single stage follower designs were found to be incapable of good fidelity of pulse reproduction, principally from a symmetry viewpoint. The necessarily lower transfer constant also resulted in excessive grid capacitance-circuit loading.

The five identical readout channels were constructed using the circuit described in Figure IX.

7. Adjustment of System Bandwidth

Previously it was noted that the signal-to-noise ratio is inversely proportional to the square of the bandwidth of the photomultiplier output circuits. Early measurements made with very wide bandwidth readout circuitry produced both disappointingly low output signal voltages and poor signal-to-noise ratio. The overall system bandwidth was inadequate as well. Reduction of photo-

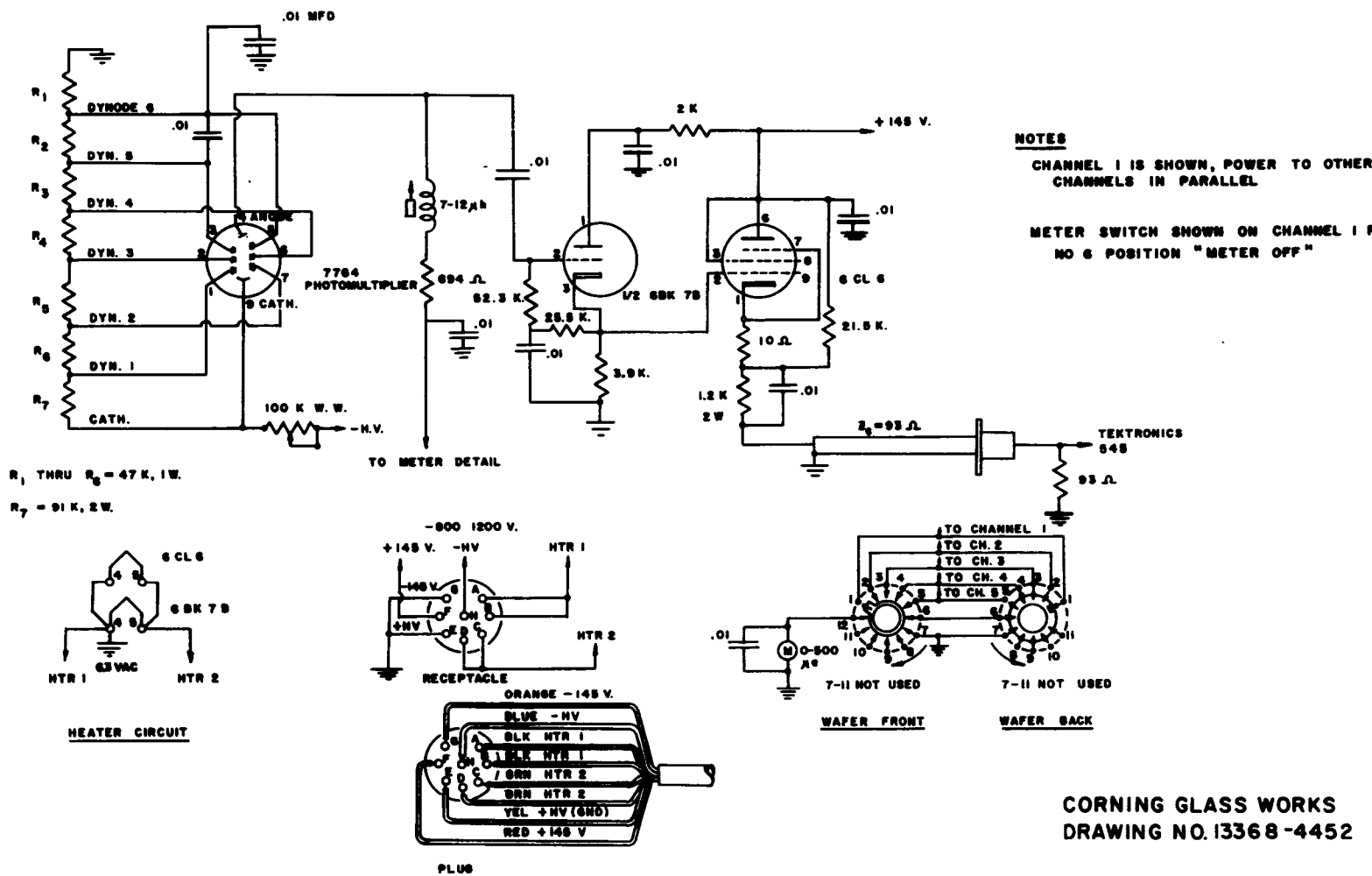

CORNING GLASS WORKS
DRAWING NO. 13368-4452

Fig. IX Photomultiplier - Cathode Follower Schematic

multiplier output bandwidth was indicated so the coupling circuit shown in Figure X was tried. Since the photomultiplier approximates a constant current generator, output signal voltage is directly proportional to anode load impedance, if the impedance is relatively low.

Resistive load impedance presented to the photomultiplier anode at 15 mc/s is approximately 2600 ohms (parallel equivalent of 694 ohm resistor). By series connecting the 694 ohm resistor with a 10 uh inductor, the rate of roll off of signal on the low frequency side of resonance is reduced. A low D. C. resistance is also desirable because it helps minimize annoying base line shifts during adjustment of the bias level of the photomultiplier.

Design bandwidth of the readout circuit was slightly over ten megacycles. The measured bandwidth was nine megacycles - less than one picofarad added capacitance can account for this difference. Bandwidth of the delay line alone was approximately 8 mc/s.

Overall system bandwidth was measured and, as expected, was found to be narrow. Bandwidths of approximately 6 mc were noted. Signal level and signal-to-noise ratios were improved however. To restore overall system bandwidth, delay line frequency compensation was employed.

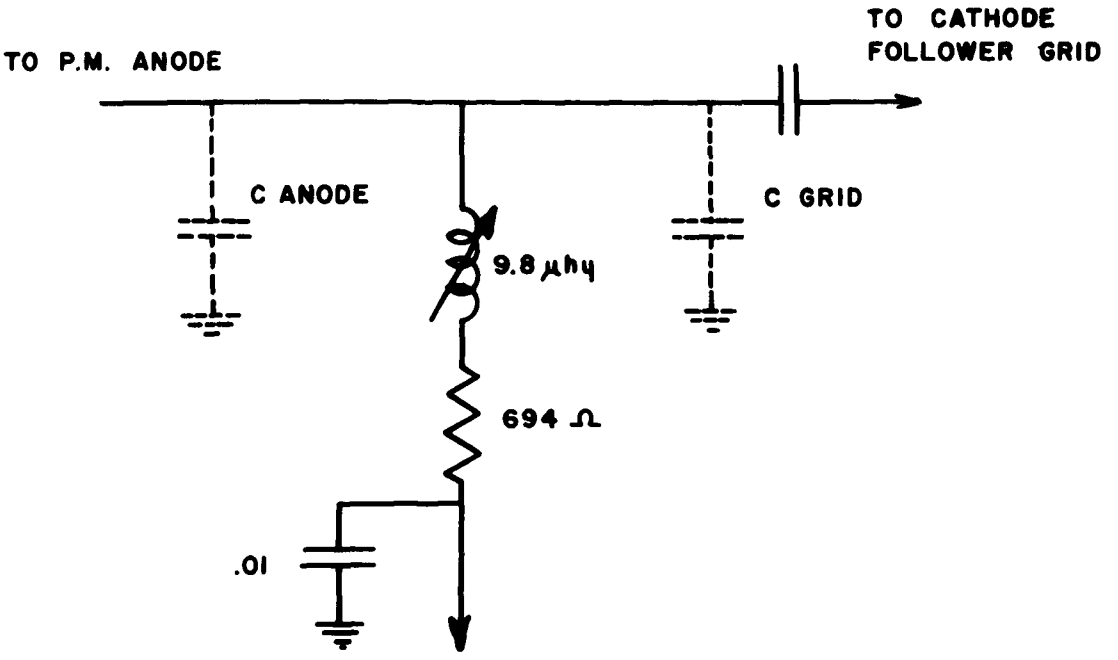

Fig. X Photomultiplier Output Coupling Circuit

A parallel RLC network was constructed and inserted in series with the ungrounded transducer lead, as shown in Figure XI. A capacitance equal to the 15 mc/s - 2000 pf transducer capacitance was selected and parallel-resonated at 15 mc/s with a miniature coil. A resistance value of ten ohms was inserted to produce the desired impedance curve, and system bandwidth was remeasured with the network in place.

The resultant bandwidth was in excess of 10 mc/s and reasonably flat, however, band-center falloff (or suckout) prompted downward adjustment of the resistance to 7.4 ohms. With this network configuration, nearly flat-topped response curves with bandwidths of 10 mc/s or more were obtained.

The d. c. photomultiplier anode current, and, therefore the output signal voltage, is determined in part by the tube gain. Sufficient light was available so that it was always possible to draw between 100 and 500 uamps. This enabled output signal voltages greater than 50 millivolts into 93 ohms.

8. Wiley Electronics Receiver and Photomultiplier

The specifications and performance of the transistorized receiver and the photomultiplier unit (Figures XII and XIII) are covered in the Wiley Electronics' Report #167, submitted with this report as Appendix B.

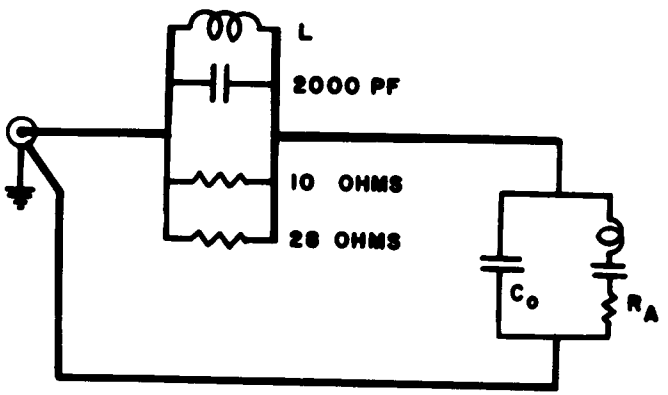

TRANSDUCER EQUIVALENT
CIRCUIT NEAR RESONANCE
$C_o \simeq 2000$ PF
$R_A \simeq 3$ OHMS

L - MINIATURE INDUCTOR
5 T - #22 HF 3/32" FORM,
SPREAD TURNS & CLIP AS REQ.
TO RESONATE 15-15.5 MC

RESISTANCES ARE TYPE S-20

CIRCUIT Q $\simeq$ 1.5

COMPONENT LEADS AS SHORT
AS POSSIBLE. HEAVY LINES
INDICATE 3/8" x 5 MIL TINNED
COPPER STRIP.

Fig. XI Input Frequency Compensating Circuit

Several advantages in using this transistorized receiver are worth considering.

The low input impedance of the receiver permits cable connection to the photomultiplier, thus remote location of the receiver is possible.

The high available receiver gain provides output signal levels in excess of 200 millivolts, as compared to the 50-60 millivolts obtained from the cathode follower circuitry.

Power consumption of the receiver is only 1.5 watts. Heater power alone for a cathode follower channel is 7 watts, or nearly five times the total transistor receiver power required.

Cubic volume and weight of the transistorized unit is estimated at 1/8 or less of the equivalent vacuum tube circuitry and could be further reduced by redesign.

These last three factors would obviously become significant considerations in the design of a multi-channel device.

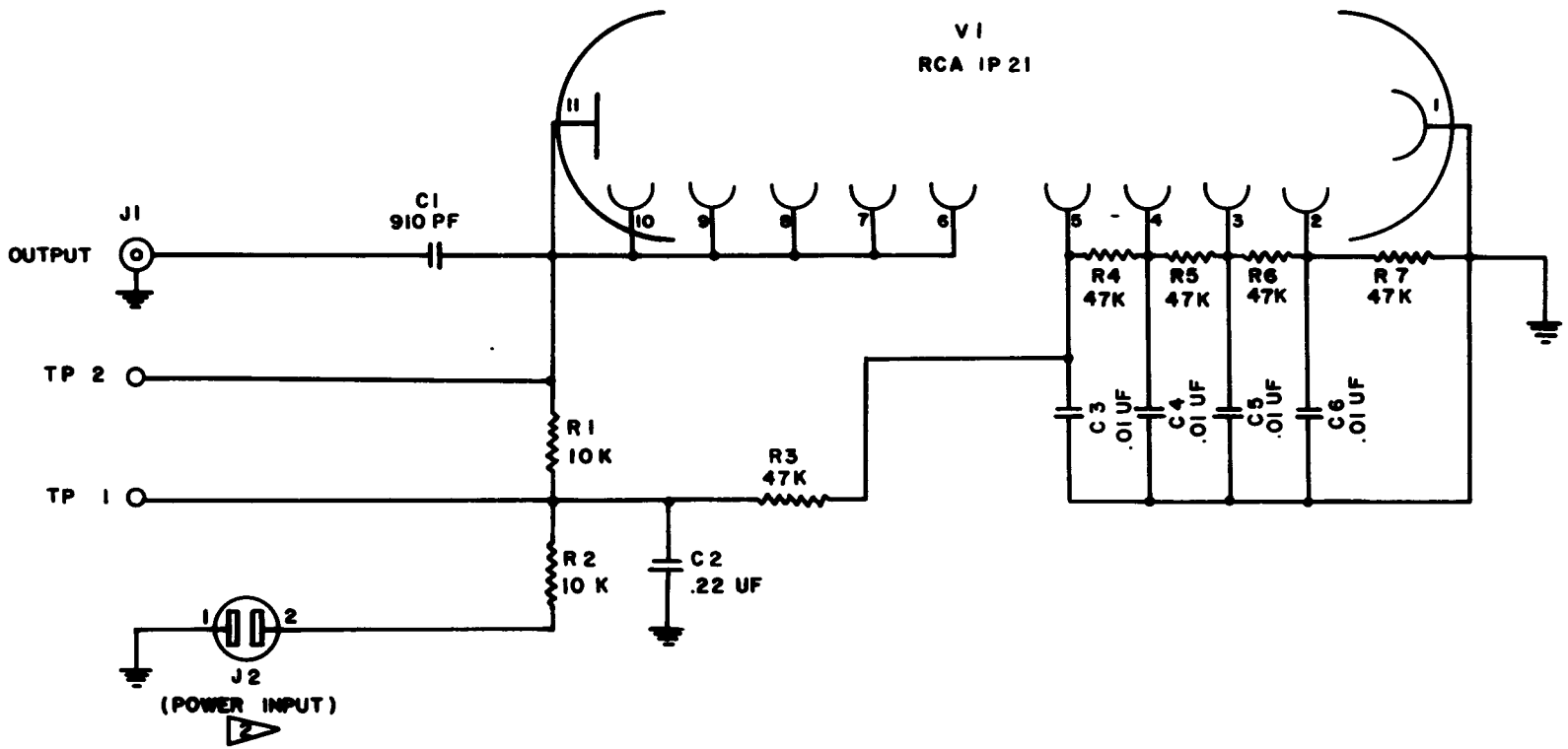

NOTES: UNLESS OTHERWISE SPECIFIED

1. ALL RESISTORS ½ W, ±10% MOLDED CARBON
2. OPERATING VOLTAGE +300 TO +500 VDC DEPENDING ON 1P21 (V1) SENSITIVITY

WILEY ELECTRONICS CO.
DRAWING NO. 1212-B-802

Fig. XII Photomultiplier Chassis Circuit

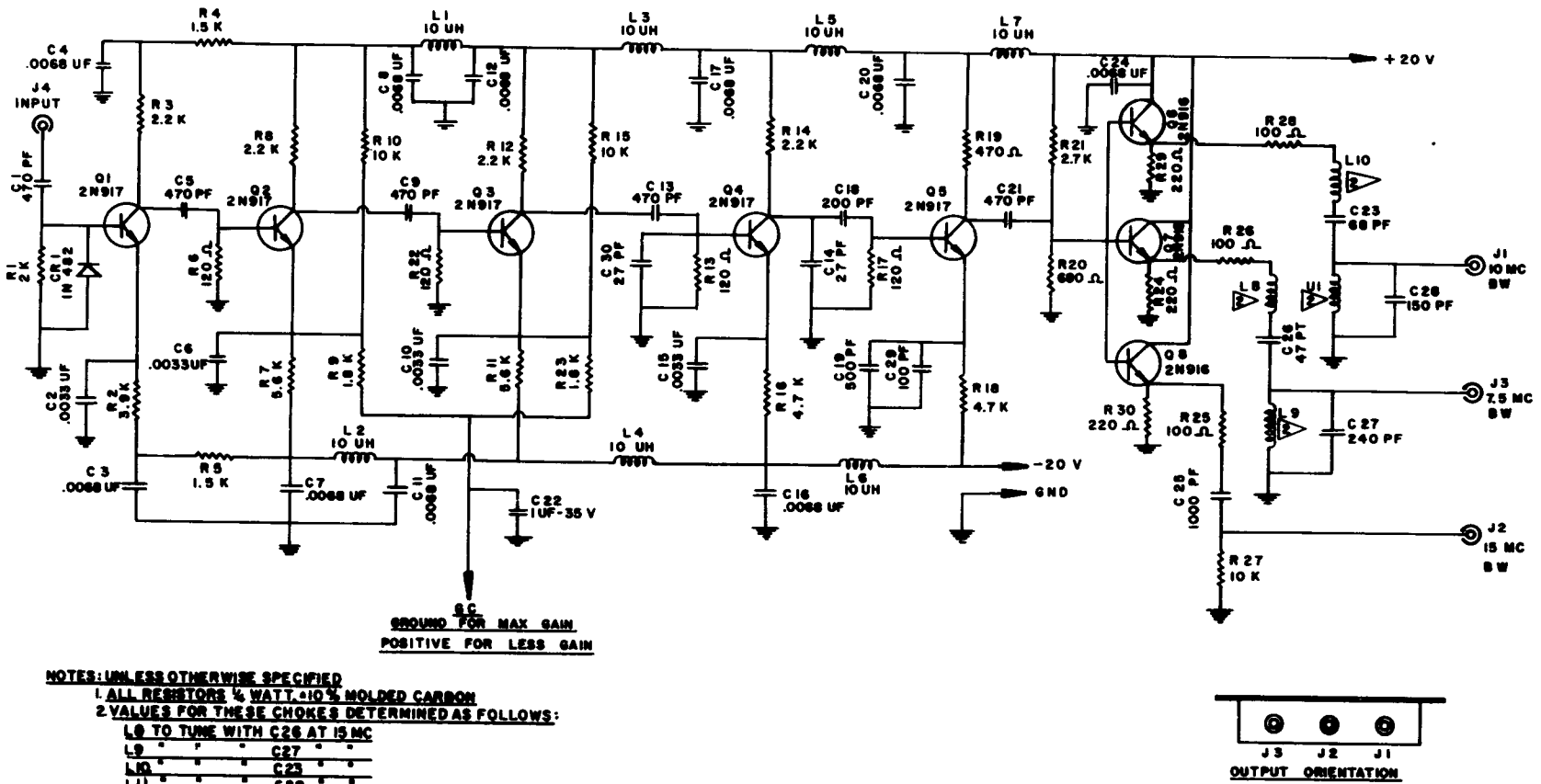

NOTES: UNLESS OTHERWISE SPECIFIED

1. ALL RESISTORS ¼ WATT, ±10% MOLDED CARBON
2. VALUES FOR THESE CHOKES DETERMINED AS FOLLOWS:
   - L8 TO TUNE WITH C26 AT 15 MC
   - L9 " " " C27 " "
   - L10 " " " C23 " "
   - L11 " " " C28 " "
3. OUTPUT JACK IN USE TO BE LOADED WITH 100 OHM RESISTANCE & 15 mmf MAX. CAPACITY IN SHUNT. UNUSED OUTPUTS TO BE UNLOADED

WILEY ELECTRONICS CO.
DRAWING NO. 1212-C-801

Fig. XIII Receiver Circuit

V CONCLUSION

A multiple tapped photoelastic delay line has been designed and constructed to fulfill the requirements outlined in part B of Section I. Indications are that the technique can be extended to provide even greater (20 mc/s) overall bandwidth, better signal-to-noise ratio (30 db over a large area or 40 db over a restricted area), and closer tap spacing (. 033 usec).

Efforts are now being directed to accomplish the above and to provide means for illuminating the full 100 usec of delay path. In addition a 30mc driver and a 30mc amplifier are under development.

The work described in subsequent reports will indicate the limitations of the technique and establish the ultimate performance that can be expected.

VI APPENDICES

A. Analysis of the Properties of the Optical Slit

Since the light modulation in a photoelastic delay line is not in phase throughout the line, it is necessary to restrict the field presented to the photocell with a slit, in order to detect the changing light intensity. The discussion which follows is a theoretical analysis of the response of the optical slit as a function of slit width.

The light intensity-phase difference characteristic in the delay line system is illustrated in the graph below. The device is usually operated in the linear region.

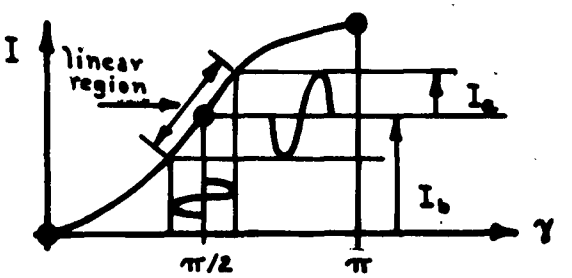

I is the intensity, and γ , the phase difference of the light components which is modulated by the stress wave in the delay line. This response characteristic applies to any point along the delay line.

In the illustration below, the light intensity along the line $\overline{SS}$, a distance r from the start of the wave is characterized by the equation: $I = I_b + I_a \sin \omega\left(t - \frac{r}{c}\right)$

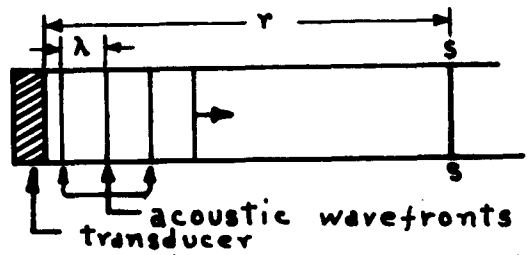

The light intensity is assumed to be the same at any point along any vertical line, which is parallel to the wavefront. I_b is the bias light intensity which is constant, i. e., independent of time and position along the line. I_a is the peak amplitude of the light, modulated by the acoustic signal in the delay line. C is the acoustic velocity of the wave and t represents time. The harmonic time dependence of the light intensity and its phase relation along the delay line is presented by the $\sin \omega\left(t - \frac{r}{c}\right)$ argument.

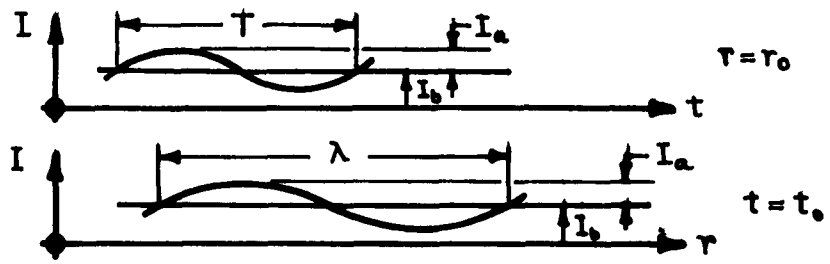

Light intensity as a function of distance r and time t along the delay line are illustrated above.

We now want to consider theoretically what response to expect by considering a slit of width δ , that is, a slit aperture whose lower and upper bounds along the line are r_1, and r_2, respectively where $\delta = r_1 - r_2$

Since the photocell is an intensity proportional device, the voltage output of the photocell is proportional to the integral of the intensity passed by the slit, that is:

$$I_t = \int_{r_1}^{r_2} \left[I_b + I_a \sin \omega \left(t - \frac{r}{c} \right) \right] dr$$

$$= I_b \delta + \frac{2 I_a c}{\omega} \sin \frac{\delta \omega}{2c} \sin \omega \left(t - \frac{r_1 + r_2}{2c} \right)$$

The $\sin \omega \left(t - \frac{r_1 + r_2}{2c} \right)$ term represents the harmonic time dependent term.

The constant bias voltage produced by the photocell is proportional to $L_b = I_b \delta$

whereas the amplitude of the modulation voltage is proportional to

$$L_a = \frac{2 I_a c}{\omega} \sin \frac{\delta \omega}{2c}$$

The modulation itself, that is, the ratio of modulation amplitude to the bias value is given by

$$m = \frac{I_a}{I_b} = \frac{I_a}{I_b} \frac{\sin\left(\frac{\delta\omega}{2c}\right)}{\left(\frac{\delta\omega}{2c}\right)} = \frac{I_a}{I_b} \frac{\sin\left(\frac{\delta\pi}{\lambda}\right)}{\left(\frac{\delta\pi}{\lambda}\right)}$$

This is plotted below versus slit width

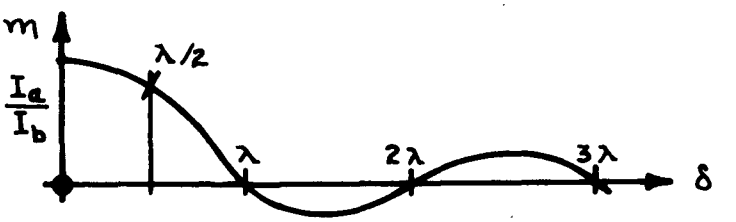

and a plot of modulation versus angular frequency is:

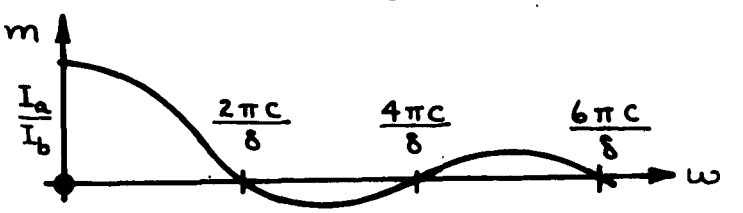

Notice that these are Fraunhofer in character.

Below is a plot of the modulation amplitude versus angular frequency :

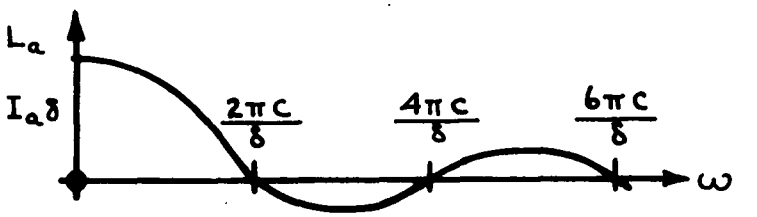

and a plot of modulation amplitude versus slit width.

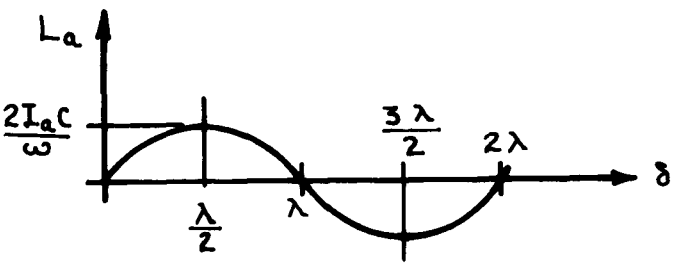

The modulation bandpass of a half wave-length slit width $\delta = \lambda_0/2$, where λ_0 corresponds to the angular frequency ω_0, is illustrated by the graph below.

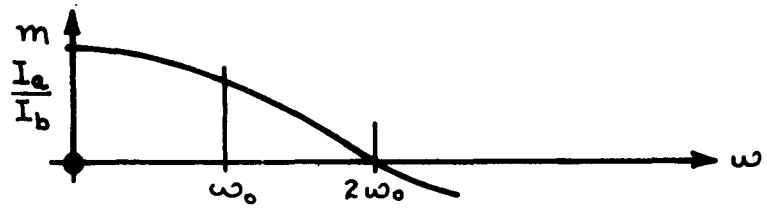

and the corresponding modulation amplitude bandpass is characterized by the following curve.

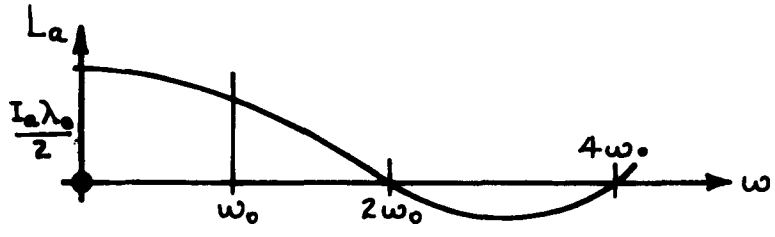

The results of this consideration indicates that:

(i) Maximum modulation is achieved by having a slit width that is infinitely small, i. e., $\delta \rightarrow 0$.

(ii) Maximum modulation amplitude is achieved by having a slit of width $\lambda/2$, i. e., half the wave length of the acoustic wave.

(iii) The bandpass due to the slit is Fraunhofer in character.

B. Test Results of An Optical Delay Line System Using the 1P21 And A Wide Band Video Amplifier

PREPARED FOR

CORNING GLASS WORKS

Bradford, Pennsylvania

Prepared by: R. K. Peterson, Project Engineer

WILEY ELECTRONICS COMPANY
2045 West Cheryl Drive
Phoenix 21, Arizona

TABLE OF CONTENTS

TABLE OF ILLUSTRATIONS

LIST OF TABLES

I. INTRODUCTION

It was presumed at the beginning of the project, that the theoretical noise performance of an optical delay line with photomultiplier pick-up could be obtained with the configuration of Figure 1.

The central idea of this arrangement was to limit the application of the photomultiplier to provide only enough gain to overcome the amplifier noise figure and no more. It was assumed that this procedure would allow a greater quantity of light to be incident on the photo cathode without exceeding the 0. 1 ma anode current rating of the multiplier. In order that the multiplier gain should be obtained with the least noise, it was planned to operate each dynode at full gain, but to utilize only the first four dynodes. The noise figure of the system should then be determined only by the theoretical noise limitation of the cathode.

Reference to Zworykin and Morton, Television, pp. 61 gives

$$i_n^2 \cong 2e(f_2 - f_1)\left(1 + \frac{\epsilon}{\sigma - 1}\right) i \sigma^K$$

where i_n is the rms noise current at the output

e is the charge on the electron

$f_2 - f_1$ is the bandwidth

ϵ is a constant taken as 1. 5

σ is the dynode multiplication factor

i is the output current (D. C.)

K is the number of active dynodes

We note that

$$i = i_0 \sigma^K$$

where i_0 is the cathode current, then (1) becomes

$$i_n^2 = 2e\Delta f \left(1 - \frac{\epsilon}{\sigma - 1}\right)\frac{i^2}{i_0}$$

or

$$\frac{i_n^2}{i^2} = \frac{N}{S} = \frac{2e\Delta f}{i_0}\left(1 - \frac{\epsilon}{\sigma - 1}\right)$$

taking the values

Δf = 1.5×10^7 cps

ϵ = 1.5

σ = 5

e = 1.6×10^{-19}

gives

$$\frac{S}{N} = \frac{i_0}{2\,(1.6)\,10^{-19}\,(1.5)\,10^7\,(1 + \frac{1.5}{4})}$$

$$= 1.33 \times 10^{11}\, i_0$$

We may express i_0 as βI_b where β is the cathode radiance in amps per lumen and I_b is the incident light in lumens. For a 1P21 and 500 μ-lumens,

$$\frac{S}{N} = 1.33 \times 10^{11} (40)\, 10^{-6}\, (500)\, 10^{-6}$$

or

$$\frac{S}{N} = 2.66 \times 10^3$$

Since this is the ratio of the noise current to the D. C. current, the result may be expressed as

$$\frac{S}{N} = 34.2 \text{ db}$$

Unfortunately, the D. C. current is not the signal in our case. For 50 percent modulation, the signal current is lessened by the ratio of the peak to peak value to the rms value, or .354 or 4.5 db. Hence, we should obtain a signal to noise ratio given by

$$\left(\frac{S}{N}\right)_o = 29.7 \text{ db} \qquad (4)$$

During the course of the measurements, it was determined that the quantity of light available was more like 2000 μ lumens and further, the 1P21 finally used had a sensitivity of 50 μ amps/lumen as opposed to forty; the measurement result, should therefore have been

$$\frac{S}{N} = 29.7 + 6 + 1 = 36 \text{ db}$$

This result will be compared with the measured values later in the report.

A second matter of interest is the comparison of the lamp spectrum of the tube with the response curve of the photomultiplier. This analysis was carried out for 2 types of tubes, the 1P21 with an S-4 cathode and the 7029 with an S-17 cathode. Figures 2 and 3 show

the results. The S-17 appears to have about twice the sensitivity of a 1P21.

II EQUIPMENT DESCRIPTION

The equipment utilized in the experiments were the following:

A. A Receiver Amplifier as per Wiley Drawing 1212-C-801, with the following specifications:

1. Noise figure - 8 db
2. Bandwidth as shown in Figure 4
3. Gain - 0 to 75 db
4. Output impedance to match 100 ohm resistive
5. Output, max. 200 mv rms
6. Required receiver current input for 40 db Signal to noise ratio - 10 μ amps

B. Two 1P21 Photomultipliers wired as shown in Wiley Drawing 1212-B-802. The sensitivities of these tubes were as follows:

#1. 10μa/lumen (estimated)

#2. 50μa/lumen, selected by RCA and certified.

The #2 tube has been supplied to Corning Glass Works.

C. The Electro-optic Delay Line and Associated Optics

The delay line was set up to be driven 10 volts peak to peak at 15 mc.

The driver was pulse operated with a 10 usec pulse. The slit was selected to be $\lambda/2$ wide at 15 mc or about 5 mils.

Various collimating lenses were employed, having focal lengths of 3 inches to 6 inches. The choice of lens was not critical.

Circular polarizer and plane polarizers were selected from several samples for best results, with considerable variation being exhibited.

III. TEST RESULTS

A. Signal to Noise Ratio

Best signal to noise figures were obtained under the following conditions:

1. Drive 10 v p - p
2. Photo anode current, .05 ma
3. Collimating lens, 4" focal length
4. Phototube 8" from line
5. Polaroids selected
6. Light collimation, slightly converging
7. Phototube #1 or #2
   Signal to noise ratio 26 db

B. Bandwidth of System

The bandwidth of the system was measured between the Driver output, (line input) and the receiver output as shown in Table I on the following page.

As can be seen, this bandwidth is less than expected. If we correct these figures for the receiver bandwidth, the results for the line and phototube alone are shown in Table II.

C. General Comments

The most significant result of the experiment was the absence of improvement in the signal to noise ratio when the improved 1P21 was used. Theoretically, the figure should have been enhanced by about 7 db, giving a signal to noise ratio of over 30 db. Secondly the value of S/N obtained would still be about 3 db below the theoretical value.

TABLE I - LINE-RECEIVER BANDWIDTH

Frequency	Relative Response
9 mc	.60
10	.65
11	.72
12	.75
13	.85
14	1.0
15	1.0
16	.90
17	.65
18	.50
19	.25
20	.10

TABLE II - BANDWIDTH OF LINE & PHOTOTUBE

Frequency	Relative Response
9 mc	.705
10	.74
11	.77
12	.78
13	.87
14	.995
15	1.00
16	.91
17	.67
18	.54
19	.28
20	.13

One possibility may explain these anomalies; namely, that the system was passing a large quantity of unmodulated light, thus yielding in fact less than 50 percent modulation, even when the correct voltages were applied to the line. The unmodulated light may arise due to the following causes:

1. Slit too wide even at 15 mc, and most certainly, at higher frequencies.
2. Portions of the light, particularly that at 4000 $\mathring{A}$ and shorter wave lengths was not suitably polarized. Reference to Figure 2 shows that nearly one-half of the light is in the region with the spectrum. Rough spectroscopic analysis bears out the curve of Figure 2, showing a large percentage of violet light from the lamp.

IV. CONCLUSIONS

1. Improved signal to noise ratios should be pursued by the following means:
   a. Narrower slit
   b. Improved optics
   c. Use of S-17 phototube or possibly other sensing devices.
2. Greater bandwidth should be pursued by means of
   a. Narrower slit
   b. Improved driver design
   c. Improved transduce performance

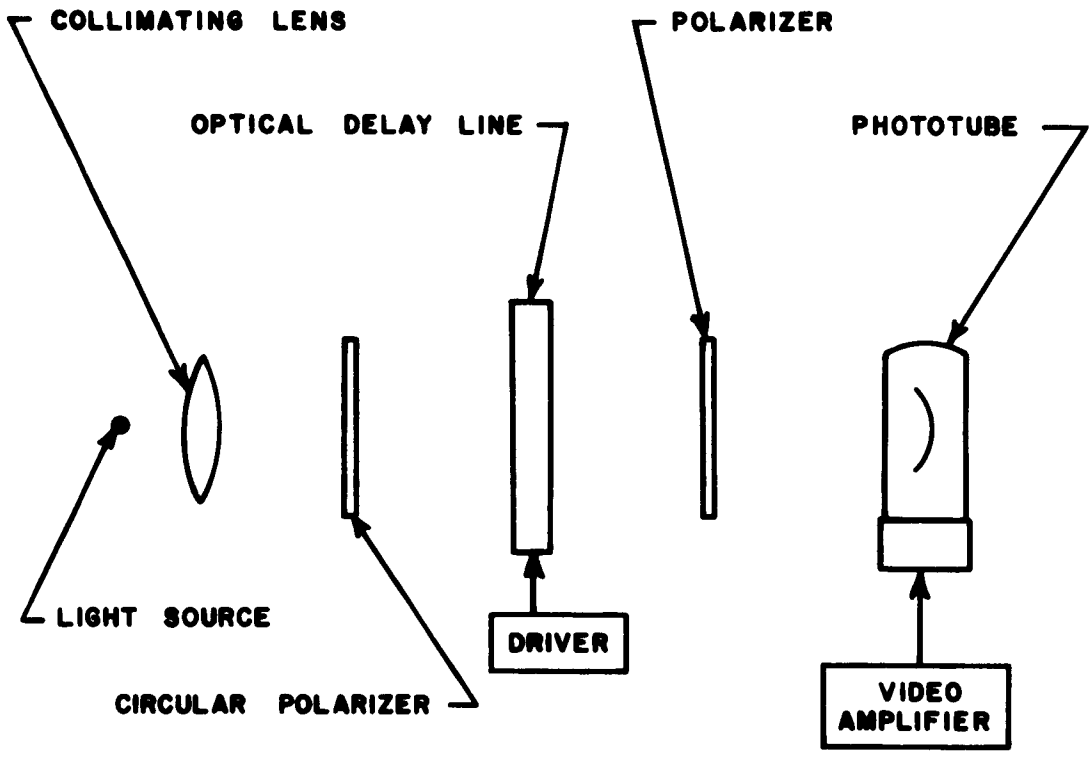

FIGURE 1

BASIC DELAY LINE SYSTEM

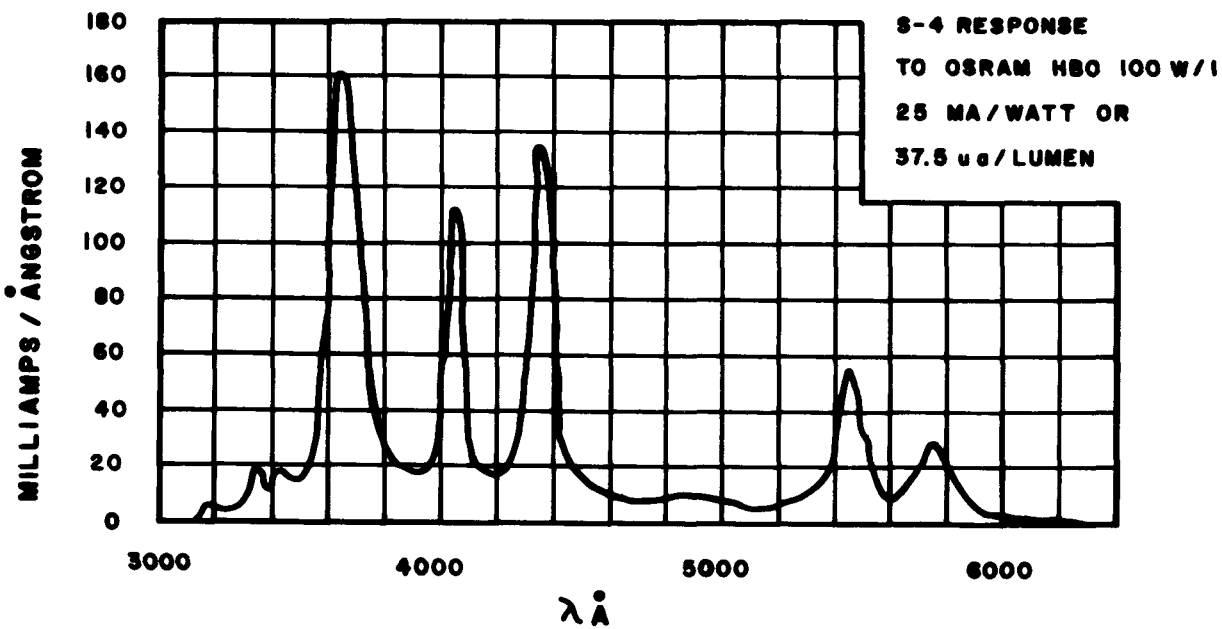

FIGURE 2
S-4 RESPONSE

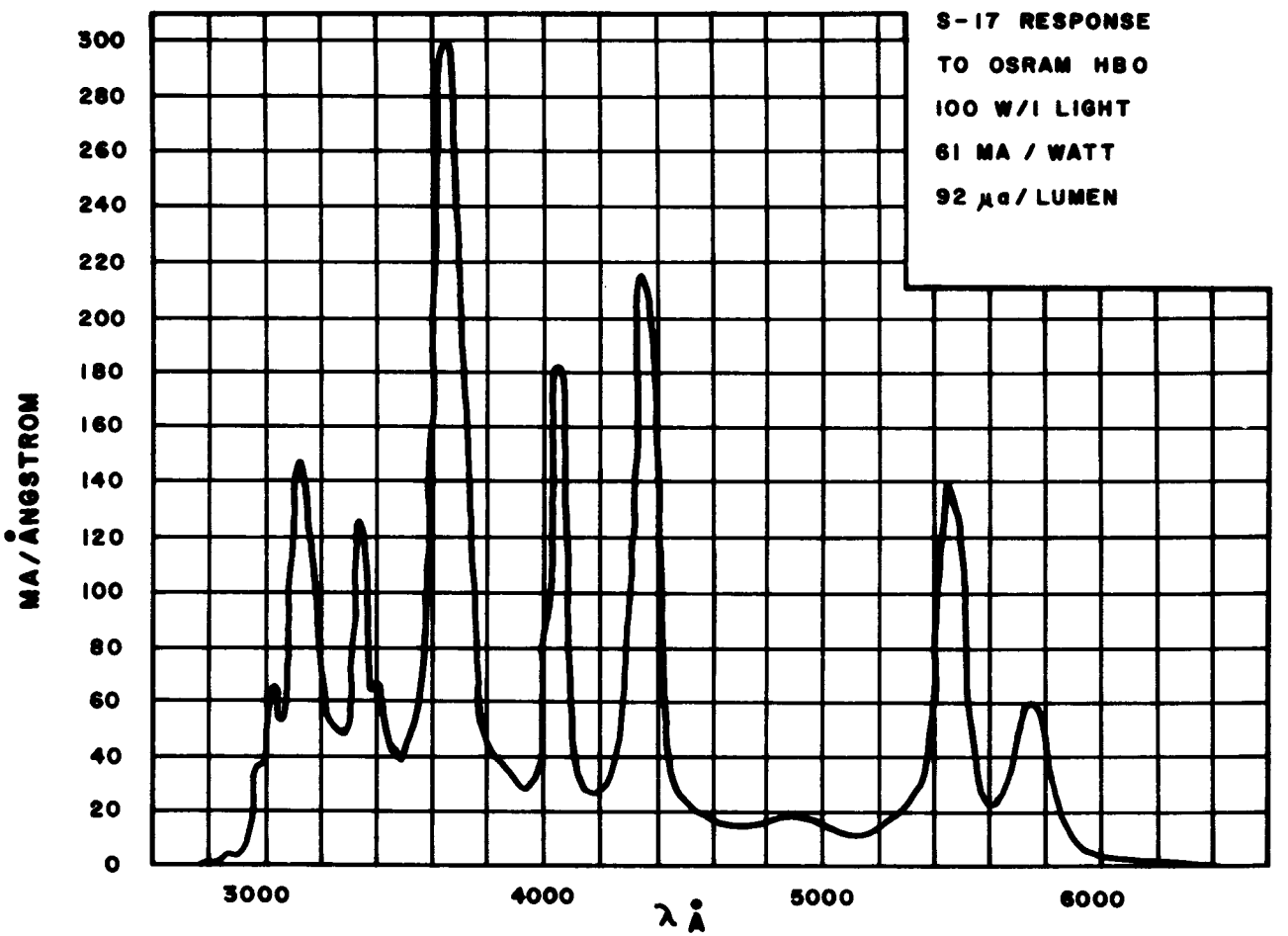

FIGURE 3
S-17 RESPONSE

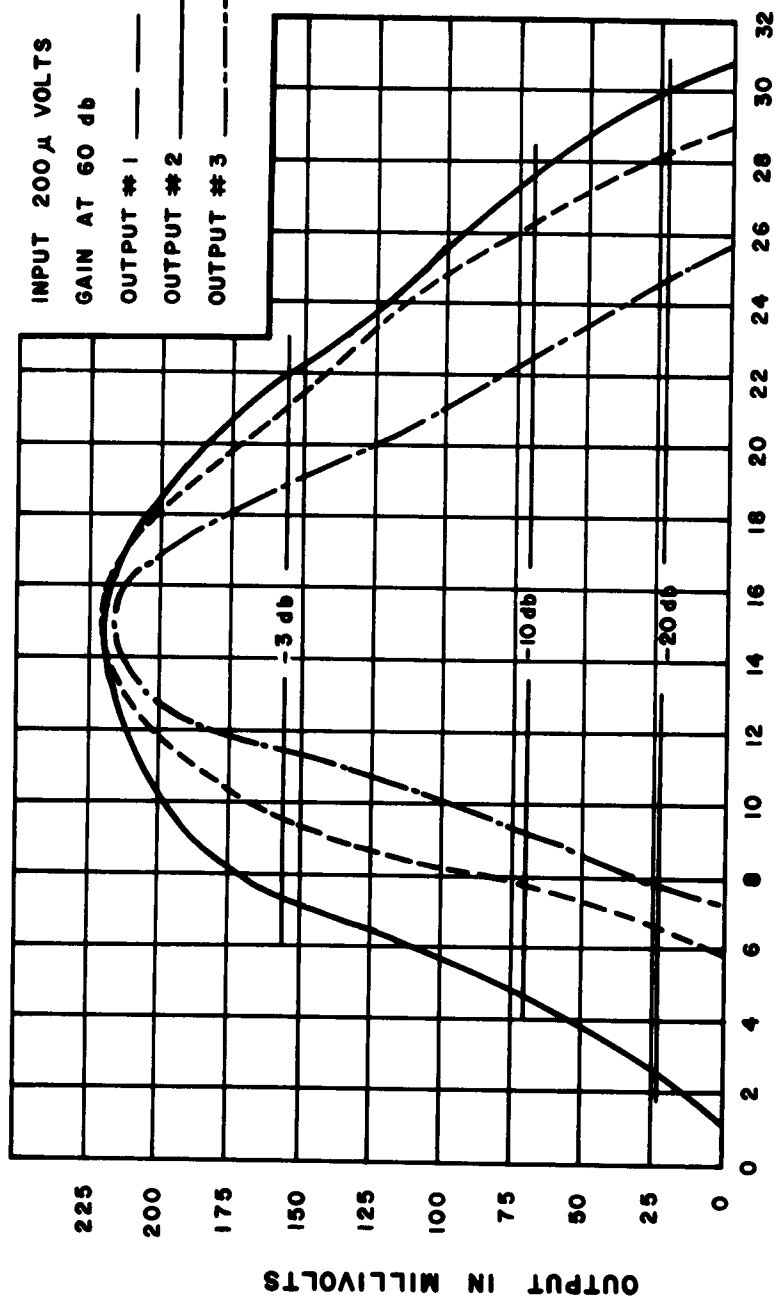

FIGURE 4
RECEIVER AMPLIFIER BANDWIDTHS

VII REFERENCES

(1) D. L. Arenberg, "Ultrasonic Solid Delay Lines", Journal Acoustical Society of America, 1, Jan. 1948, pp. 1-26.

(2) R. W. Wilmotte,"Instantaneous Cross-Correlation", Final Report, Sept. 1957, RADC Contract No. AF 30 (602)-1494, ASTIA NO. 215 485.

(3) H. A. Brouneus and W. H. Jenkins, "Photoelastic Ultrasonic Delay Lines", Proceedings of the National Electronic Conference, October 1960, pp. 835-839.

(4) Jenkins and White, Fundamentals of Optics, McGraw-Hill Book Co., Inc. 1950.

(5) Zworykin and Morton, Television pp. 61.